Counter-Misdirection in Behavior-based Multi-robot Teams *

Shengkang Chen, *Graduate Student Member, IEEE* and Ronald C. Arkin, *Fellow, IEEE*

***Abstract*—When teams of mobile robots are tasked with different goals in a competitive environment, misdirection and counter-misdirection can provide significant advantages. Researchers have studied different misdirection methods but the number of approaches on counter-misdirection for multi-robot systems is still limited. In this work, a novel counter-misdirection approach for behavior-based multi-robot teams is developed by deploying a new type of agent: counter misdirection agents (CMAs). These agents can detect the misdirection process and "push back" the misdirected agents collaboratively to stop the misdirection process. This approach has been implemented not only in simulation for various conditions, but also on a physical robotic testbed to study its effectiveness. It shows that this approach can stop the misdirection process effectively with a sufficient number of CMAs. This novel counter-misdirection approach can potentially be applied to different competitive scenarios such as military and sports applications.**

I. Introduction

Humans and Animals commonly use deception to provide benefits or advantages for themselves. For instance, blue jays can mimic the sound of hawks to scatter other birds in the area so that they will have fewer competitors for food [1]. In the same manner, with the growth of robotic intelligence, applying deceptive behaviors may be beneficial to robotic systems. For example, robots could deceive others including humans or other robots by sending inaccurate or falsified information purposely. This concept is known as robotic misdirection -- robots misleading other agents to the wrong location that may be traps or other remote locations to gain advantage over them. To counter this misdirection, robotic counter-misdirection strives to stop this misdirection process or negate its effects. Although studies on robotic misdirection [1]–[3] exist, the field of robotic counter-misdirection has been understudied.

In a competitive multi-robot environment such as competitions, some robots can use misdirection techniques to provide them with an edge over others to accomplish their goals. As a result, counter-misdirection becomes crucial for these misdirected robots. Two main components in counter-misdirection include misdirection detection and misdirection stoppage. Based on these two main components, a new type of agent called counter-misdirection agent (CMA) is presented. These agents detect the misdirection process by observing misdirected agents' movements and then forming a "barrier" to stop them.

The main contributions of this research involve providing a misdirection/counter-misdirection framework for behavior-based multi-robot systems and developing a counter-misdirection approach using a novel type of behavior-based robot agents: counter-misdirection agents (CMAs).

II. Background

A. Robot Deception

Robotic deception can be interpreted as robots using motions and communication to convey false information or conceal true information [4],[5]. Deceptive behaviors can have a wide range of applications from military [6] to sports [7]. Researchers have studied robotic deception previously [4] through computational approaches [8] in a wide range of areas from human–robot interaction (HRI) [9]–[11] to ethical issues [4]. Shim and Arkin [5] proposed a taxonomy of robot deception with three basic dimensions: interaction object, interaction goal and interaction type. This taxonomy provides a basic metric of robot deception. Based on this taxonomy, they [6] developed a computational framework to allow the robot's deceptive actions to benefit human users. This work was extended to a scenario where robots act deceptively to control victims' fear and shock in search and rescue [7]. Additionally, they [8] have shown that robots can model deceptive behavior from small animals. Inspired by the caching behavior of a squirrel, a robotic deceptive strategy was developed. Instead of going directly to the caching location, the robot moved between the actual caching location and the fake locations in order to confuse competing robots. Furthermore, in human–robot interaction (HRI), researchers have studied deception in robot motion context. Srinivasa's team analyzed and classified different deceptive robot motions used to approach different goal areas [4].

While most research on robotic deception has focused on single robotic systems, few studies considered multi-robot systems. Arkin's group is one of the few research groups that studied deception in multi-robot teams. Earlier their research involved studying mobbing behavior where birds harass a predator for deterrence, resulting in a deceptive model for multi-robot systems [9]. While this deceptive model was designed specifically for predator deterrence, the misdirection framework of this paper is intended for group movement misdirection scenarios.

B. Group Behaviors in Multi-robot Teams

Multi-robot teams are modeled using group behaviors for different purposes and scenarios. For example, lekking behavior from birds has been implemented in multi-robot teams for multi-robot groups [10] where members from a multi-robot team follow the leader of the team while

* Research supported by the National Science Foundation under CNS EAGER grant #1848653.

S. Chen is in Electrical and Computer Engineering, R.C. Arkin is in Interactive Computing, Georgia Institute of Technology, Atlanta, GA 30308, USA (e-mail: schen754/arkin@gatech.edu).

maintaining a certain distance. To model the flocking behaviors of animals, the selfish herd model [11] and the Boids model [12], [13] were proposed. Selfish herd model [11] is used to mimic a flocking behaviors of a group of sheep or ducks. Similar to the selfish herd model, the Boids model [12], [13] which tries to mimic the behavior of a flock of birds, enables agents to stay close to nearby agents without collision. Another group behavior model uses the threshold model [14], which models the behavior of a crowd of people. When the number of nearby individuals that engage in a similar action exceeds the "threshold" for a nearby individual, this agent will likely undertake this action as well.

Robots have been used to drive animals to designated locations or divert them away from certain locations based on their natural flocking behaviors [15]–[18]. Vanghan et al. [16], [18] used a robot as a sheepdog to herd ducks to a desired location. Strombom et al. [15] proposed a 2-step algorithm to drive unwilling agents to move in the same direction using a single agent. Researchers have also studied diverting flocks of birds from airports [19], [20] using the Boids model for the birds. These methods are considered fear-based 'push' approaches where robots act as predators to force animals to move away from the shepherding robots.

Based on the threshold model, Pettinati and Arkin [2] developed an alternative "pull" approach that attracts target agents toward the goal area. Compared with the "push" method which requires at least one agent to act as a predator, the "pull" method deploys shills which are embedded among the mark (target) agents to misdirect them to the goal area.

C. *Robotic Misdirection*

Misdirection is one of the main forms of deception which can influence the attentions or movements of an agent. Magicians often use misdirection in order to create a magical effect. As a result, misdirection has been an interesting area to study in the field of psychology. Psychologists and magicians have developed different taxonomies for misdirection [21]. Among them, Lamont and Wiseman's taxonomy from their book "Magic in Theory" [22] can be considered for the study of robotic misdirection.

Lamont and Wiseman classified misdirection into *physical* misdirection and *psychological* misdirection. Under *physical* misdirection is commonly divided into three categories: *passive* misdirection, *active* misdirection and *temporal* misdirection. Given a scenario where robots need to move to their goal area using misdirection, an example of *passive* misdirection is where robots use camouflage to avoid detection while moving to their goal area; similarly, *active* misdirection is when robots move oddly to attract attention so that other confederate robots can move to their goal area secretly; and *temporal* misdirection is where robots wait a long period of time until they are no longer being "watched" before they move to their goal area.

In [2] and[23], an *active* misdirection tactic was developed to "pull" a group of agents toward the goal location in contrast to the fear-based "push" methods. This research uses a "pull" threshold model [14] for a multi-robot team. By using a team of shills that move with intention, characterized by their high linear velocity movement in a common direction with small directional changes, this induces mark agents with low group following thresholds to follow the shills. In this manner, mark agents with higher thresholds will also follow as the number of agents, including the newly recruited lower threshold marks, that move with intention increases. This paper reports on research that counteracts this earlier approach [23], since in addition to the *active* misdirection tactics utilized earlier, counter-misdirection strategies are now investigated to halt or reduce the induced misdirection.

III. MODEL

In our misdirection and counter-misdirection simulation scenarios, each agent can move in a two-dimensional space and $\overrightarrow{l_{i,t}} = [x_{i,t}, y_{i,t}]$ represents agent i's location at time t with a limited observation range r_i. In the behavior-based approach [24], the movement of each agent is based on its motion vector from the current behavior assemblage: $\overrightarrow{l_{i,t+1}} = \overrightarrow{l_{i,t}} + \overrightarrow{v_{i,t}} * \delta t$ where δt is the time step. The motion vector $\overrightarrow{v_{i,t}}$ is the weighted sum of behavior vectors provided by the primitive behaviors from the current behavior assemblage: $\overrightarrow{v_{i,t}} = \sum_{j \in E_i} \rho_j \overrightarrow{b_j}$ where E_i is the set of all composing primitive behaviors and $\overrightarrow{b_j}$ is the behavior vector of primitive behaviors with gain ρ_j. The definition of each primitive behavior is described in Appendix I.

There are four types of robot agents: mark, shill, leader and counter-misdirection agent (CMA). These agents can be divided into three different groups:

- **Mark group**: a group of marks which is targeted to be misdirected, i.e., to be moved to a location not of their own choosing..
- **Misdirection team**: a team composed of a leader and a certain number of shills with the intention to misdirect marks to their goal area.
- **Counter-misdirection team**: a team composed of counter-misdirection agents (CMAs) with the goal of preventing marks from being misdirected.

This work follows from [23] which developed a misdirection approach for a multi-agent team. The goal of this new research is to develop a counter-misdirection approach. As a result, the behaviors of the misdirection leader and its shills remain the same. Moreover, this misdirection team has no knowledge of the counter-misdirection agents (CMAs). The behavioral assemblages for the different types of agents are summarized in TABLE I.

A. *Marks*

The mark agents resemble the general public or a flock of animals which can potentially be misled or stopped. Mark agents cannot distinguish between different types of robotic agents and treat every agent similarly. The Granovetter threshold model was implemented on these agents based on their collective behavior [14], where individuals of a group have a tendency to follow when they observe other members who "move with intensions." In this threshold model, if the number of observed agents which move with intentions, exceeds the mark agent's threshold $\sum_{j:|\overrightarrow{l_{i,t}} - \overrightarrow{l_{j,t}}|<R_{sensor}} \left[|\overrightarrow{v_{j,t}}| > v_{limit} \right] < \theta_i$, where R_{sensor} is the sensor range and θ_i is the threshold of agent i, the mark will then follow these agents using a Lek Behavior [10] (**Mark Flock**). Otherwise, the mark will keep wandering or simply milling about (**Mark Wander**). Here, an agent is defined as moving with intention when the agent exceeds a certain velocity threshold and is then termed an "active" agent. These mark agents can also be "pushed" by some agents using the fear-based approach [15]–[18]. The *Color-Pushed-Back* behavior enables marks to evade agents with a predefined color that are treated as predators. This feature is used by the counter misdirection agents (CMAs) to stop or inhibit an ongoing misdirection process.

B. Shills and Their Leader

Shills and their leader form a misdirection team with the goal to misdirect mark agents to a goal location. Before the leader issues a signal to start misdirection, the shills execute the same behavior assemblage as the mark agents while they are near the start location (**Wander Near Start**) to "blend in". After the leader gives the signal notifying the shills to start misdirection, the leader agent moves with intention towards its goal location with a small degree of random movement generated by the *Wander Behavior* while the shills will follow the leader (**Shill Flock**) in order to "draw" mark agents to follow them, thus achieving misdirection. This process is described in detail in [31].

C. Counter-Misdirection Agents (CMAs)

Counter-misdirection agents are deployed to deter marked agents from misdirection. Similar to marks, CMAs are not able to identify shills and their leader from marks. Moreover, since the information of the goal location is only available to the misdirection team, CMAs have no knowledge on where the leader's goal location is. The general counter-misdirection strategy for CMAs involves treating every non-CMA agent as a mark and blocking them as a group when they are misdirected. Figure 1. depicts how a CMA first wanders just like other agents at the beginning of a scenario (**Wander Near Start**). Once the number of active agents moving with the leader exceeds its own threshold, it monitors the movements of these active agents that are within its observation range for a period a time (**Observe Movement**). Then, the CMA will estimate an intercept position in front of the marks in motion based on the collective movement of these active agents (**Estimate Intercept Location**). The CMA then moves to the intercept position (and changes its color in the simulation to black indicating it is actively countering misdirection) to push mark agents away from its position to prevent them from reaching the leader's target location (**Goto Intercept Location**). Since the CMAs can only "push" the mark agents back but not the shills or their leader, these CMAs 'filter' (like a sieve) the marks from the shill team. The counter-misdirection algorithm is summarized in Algorithm 1 from Appendix II.

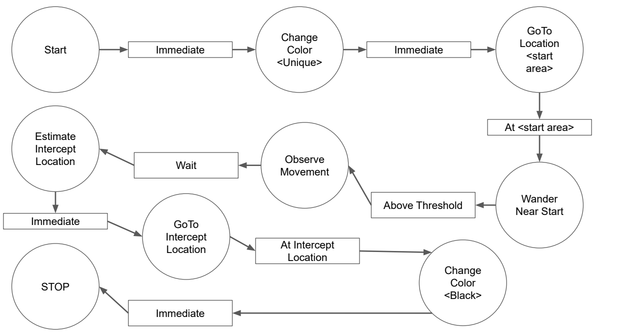

Figure 1. The FSA of a counter-misdirection agent (CMA)

In order to stop the misdirected mark agents, CMAs need to move ahead of these agents and "push" them back. Each CMA needs to predict the general movement of these agents in order to estimate the intercept location $\vec{\iota} = [i_x, i_y]$ahead of the group. During movement observation, the location of each observed agent i at each time stamp t is treated as a data point $\overrightarrow{l_{\iota,t}} = [x_{i,t}, y_{i,t}]$. After a sufficient number of data points are collected for a period of time T to generate a dataset D, it will be used for location estimation.

Based on the assumptions that the leader moves toward the designated location directly with limited wandering (noise), and that all shills will follow the leader, and that these active (high velocity) mark agents will follow other observed active agents, it is reasonable to model the group movement as a linear model.

In the local frame of the CMA, let $\vec{c} = [a, b]^T$ be the centroid of the misdirected group with the movement vector $\vec{f} = [f_x, f_y]^T$. Given the maximum speed that the CMA can achieve v_{max}, we can formulate a set of equations to solve for $\vec{g} = [g_x, g_y]^T$, the movement vector of the CMA which will allow it to intercept the misdirected group after m time units.

$$\begin{cases} \vec{c} + m\vec{f} = m\vec{g} \\ \|\vec{g}\| \leq v_{max}. \end{cases} \quad (1)$$

Assuming β is fixed, we can derive (1) into a quadratic function and solve for a positive m:

$$(a + mf_x)^2 + (b + mf_y)^2 = m^2 \beta v_{max}{}^2 \quad (2)$$

After m is found, we can easily calculate $\vec{g}$ using (1) and the intercept location $\vec{\iota} = \mathrm{m}\vec{g}$.

Once the intercept location is created, each CMA moves toward its computed intercept position. After the CMA reaches the intercept location, it will change its color to black in the simulation indicating it is signaling to repel the deceived mark agents. This behavior creates a circular effective vector field radius R_e pushing any mark agents using the *color-pushed-back* behavior.

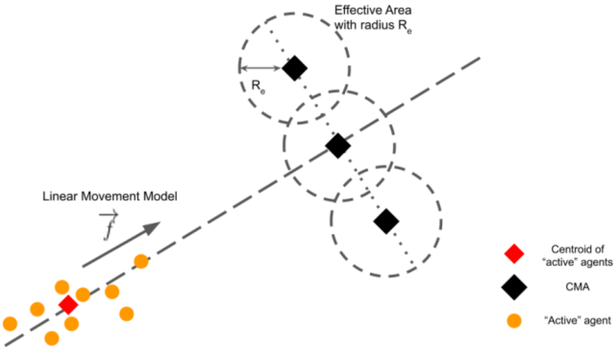

Figure 2. Diagram of the counter-misdirection deployment

In the case of more than one CMA being deployed, their estimated intercept locations for each individual agent may be very close to each other, which will be inefficient for counter-misdirection since there will be many overlapping repulsive field areas. In order to minimize the misdirection rate for counter misdirection, CMAs will try to form a "barrier" to deter the misdirected marks. As a result, each CMA relocates some distance above or below its original intercept location that is perpendicular to the group movement vector $\vec{f}$ based on an offset γ. In addition, CMAs can be "pushed" by other black colored CMAs in the directions that are perpendicular to the group movement vector $\vec{f}$ for better distribution from the *Color-Pushed-Back* behavior. This enables CMAs to form a barrier against the misdirected group of agents to achieve better counter-misdirection efficiency as shown in Figure 2. No explicit communication between CMAs is needed to achieve this separation.

IV. EXPERIMENT

In order to test the viability and efficiency of the counter-misdirection strategy by the CMAs, various cases were implemented using the *MissionLab* mission specification software system [25], which is a powerful platform designed specifically for multi-agent behavior-based systems. For each case, there is a shill team composed of a leader and two shills, a group of marks and a team of CMAs.

A. Simulation Results

A two-dimensional 60 meters by 240 meters simulation environment was created: a start area at (20, 40) with 10 meters radius and a goal area at (220, 40) with 10 meters radius as well. In the environment, each scenario was tested with 50 experiment trials for each case to analyze the performances of the counter-misdirection strategy. The misdirection rate was defined as the percentage of the marks that were misdirected to the goal area by the shill team within 360 simulation time steps.

One of the most important factors of the counter-misdirection strategy is the number of CMAs deployed. As shown in Figure 4. without the presence of any CMAs, marks were always misdirected to the goal area (misdirection rate = 1). However, as more CMAs were deployed, fewer marks were misdirected. Specifically, when the CMAs are more than 1, less than 25% of the mark agents reach the goal area. The main reason the misdirection rate is fairly high when there was only one CMA agent is due to the ratio between the radius of CMA's effective field (16[m]) and the mark's follow range (30 [m]) in the *lek* behavior. Since their follow range is almost twice as large as the CMA's effective radius, these misdirected marks can still circumnavigate the repulsive field and follow shills to the goal area if the estimated intercept location is slightly away from the misdirected marks' actual paths. In the case of multiple CMAs, these CMAs used effective fields to build a long overlapping barrier collectively (shown in Figure 3.), which makes it much more challenging for misdirected marks to follow shills. This demonstrates the effectiveness of the CMA strategy.

The main factor contributing to the case when CMAs failed to stop the misdirected marks from reaching the goal was incorrect intercept location estimation. Due to the random movement of the leader and the interactions between agents from their composing behaviors, CMAs' estimation on the movement vector of the misdirection group could be imprecise, which led to incorrect intercept location estimation. In this case, the barrier formed by the CMAs would have little overlap areas with the marks' actual paths. As a result, these misdirected marks can circumnavigate the barrier easily. This is also the reason why deploying multiple CMAs wouldn't increase misdirected marks' time to reach the goal area.

Another factor worth looking into is the inter-robot distance. Each robot has a repulsion sphere in the *off-robot* behavior for collision avoidance. As the radius of the repulsion sphere increases, robots will stay further away from other robots, which yields larger inter-robot separation. This can represent different practical scenarios: smaller inter-robot distance can represent a more crowded environment and larger inter-robot distance can represent a sparser environment. In order to investigate the effects of inter-robot distances on the counter-misdirection, the approach was tested with different numbers of CMAs and different inter-robot distances from 2 meters up to 6 meters in the simulation environment. Despite having different inter-robot distances (shown in Figure 4.), this approach is still effective on lowering the misdirection rate using a sufficient number of CMAs.

In this counter-misdirection approach, CMAs estimate their intercept locations based on the linear model (misdirected marks and the shill team move linearly toward the goal area). However, as the gain of the leader's random movement (noise) increases, instead of moving directly to the goal area, the leader moves toward different directions more frequently followed by shills and misdirected marks. This made CMA's linear-based estimation less accurate which led to higher misdirection rates as shown in Figure 6. When the random movement gain increases, it shows a significant increase on the misdirection rate even with the increase number of CMAs. Currently, this is the main limitation for the counter-misdirection strategy. It potentially can be considered a strategy for counter-counter misdirection by the leader agent.

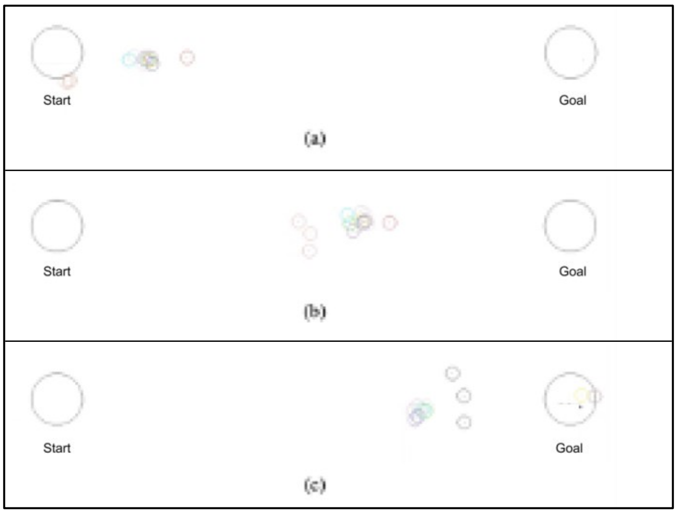

Figure 3. Screenshots of the counter-misdirection process on MissionLab: (a) CMAs (red circles near InitialArea) were observing the active agents to estimate their intercept locations; (b) CMAs were moving toward their estimated intercept locations; and (c) CMAs reached their estimated intercept locations and started deploying their effective fields (change their color to black) to push back the misdirected marks while shills and their leader were reaching the goal area without misdirecting the marks.

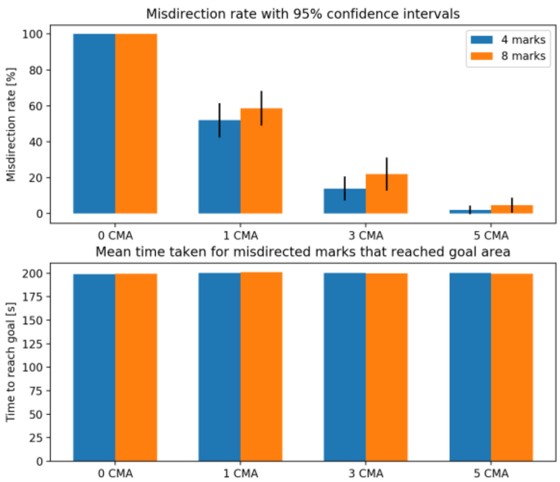

		0 CMA Mean (STD)	1 CMA Mean (STD)	3 CMAs Mean (STD)	5 CMAs Mean (STD)
4 Marks	Misdirection rate [%]	100.0 (0.0)	52.0 (48.9)	13.9 (34.2)	2.0 (12.1)
	Reach goal time [s]	199.32 (0.597)	200.18 (5.077)	200.43 (5.538)	200.20 (0.6)
8 Marks	Misdirection rate [%]	100.0 (0.0)	58.6 (48.9)	22.0 (47.5)	4.7 (20.9)
	Reach Goal time [s]	199.67 (0.613)	200.99 (7.344)	199.75 (0.476)	199.51 (0.590)

Figure 4. This shows how different numbers of counter-misdirection agents (CMAs) affect the the percentage of marks that are misdirected to the goal area by the shills (misdirection rate) along with the time taken for successfully misdirected marks that reached the goal area in both the 4 marks and 8 marks scenarios.

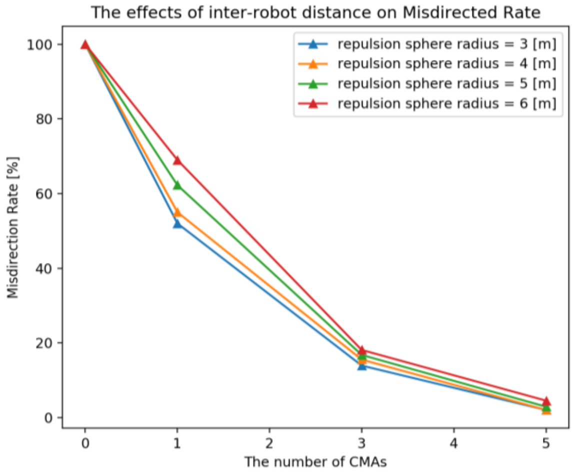

Size of the repel sphere [m]	0 CMA Mean (STD)	1 CMA Mean (STD)	3 CMAs Mean (STD)	5 CMAs Mean (STD)
3	100.0 (0.0)	52.0 (48.9)	13.9 (34.2)	2.0 (12.1)
4	100.0 (0.0)	55 (48.8)	15.5 (35.5)	2.0 (14.0)
5	100.0 (0.0)	62.3 (47.7)	16.8 (37.0)	2.8 (15.1)
6	100.0 (0.0)	69.0 (45.8)	18.1 (38.2)	4.5 (20.5)

Figure 5. This figure shows the differences in robot's repulsion sphere size where larger repulsion spheres create larger inter-robot distances which impacts the percentage of marks that are misdirected to the goal area (misdirection rate).

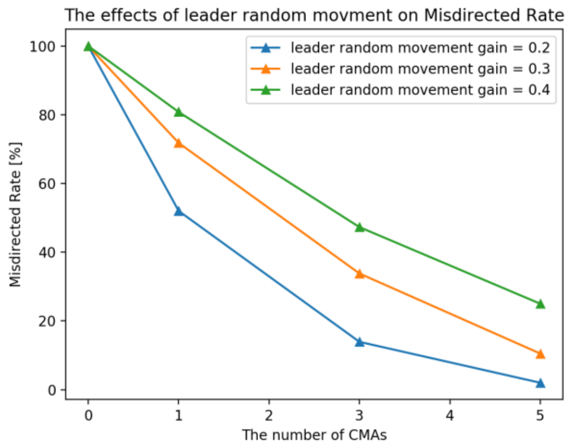

Random movement gain	0 CMA Mean (STD)	1 CMA Mean (STD)	3 CMAs Mean (STD)	5 CMAs Mean (STD)
0.2	100.0 (0.0)	52.0 (48.9)	13.9 (34.2)	2.0 (12.1)
0.3	100.0 (0.0)	71.8 (44.0)	33.8 (46.4)	10.5 (30.2)
0.4	100.0 (0.0)	80.8 (39.2)	47.3 (49.7)	25.0 (43.3)

Figure 6. This shows how the behavior gain of the leader's random movement affects the efficiency of the counter-misdirection strategy on stopping misdirected marks from reaching the goal area.

B. *Demonstration on Hardware*

The counter-misdirection strategy has been implemented on physical robots using the Georgia Tech Robotarium [26], an open-access robotics research platform. The parameters of robotic behaviors are adjusted to the smaller testing environments. Three representative trials were run with different numbers of CMAs (counter-misdirection agents): no CMA, one CMA and three CMAs. Moreover, each trial includes four marks, two shills and one leader. As expected, the same type of dynamic is observed in the Robotarium as in the simulation. The videos of these trials are available online[1].

With three CMAs deployed for counter-misdirection, these CMAs were able to stop the misdirection process by preventing the misdirected marks from reaching goal area. Once the misdirection process was detected, each CMA moved to its intercept location after movement observation and intercept location calculation were completed. After the CMA reached their intercept locations, they started to “push” misdirected marks away from their locations to stop the misdirection process. Snapshots from this trial are shown in Figure 7.

V. DISCUSSION

From these results, the following observations can be made:

As more CMAs (counter misdirection agents) are deployed, this counter misdirection approach can lower the misdirection rate substantially.

When there are more CMAs, they can form a larger barrier collaboratively which makes it harder for misdirected marks to bypass them. An important benefit of deploying many CMAs is even when some of the CMAs have incorrect estimations on intercept locations, other CMAs can still form a "barrier" to stop the misdirected marks.

The counter-misdirection approach is suitable for variable numbers of marks and different inter-robot distances.

Based on the behaviors of the marks, misdirected marks follow nearby active (high velocity) agents including other misdirected marks and shills. This makes them behave as a flock following the leader. As long as the barrier size is larger than the flock size, the counter-misdirection strategy is still effective.

The leader's random movements significantly affect the efficiency of the counter-misdirection strategy.

As the gain of the leader's random movement increases, the flock of the following shills and misdirected marks will have a less direct movement pattern toward the goal area, which makes it more challenging for CMAs to estimate the intercept locations. As a result, the counter-misdirection strategy will be less effective. This zig-zagging can potential serve as a counter-counter misdirection strategy by the leader agent.

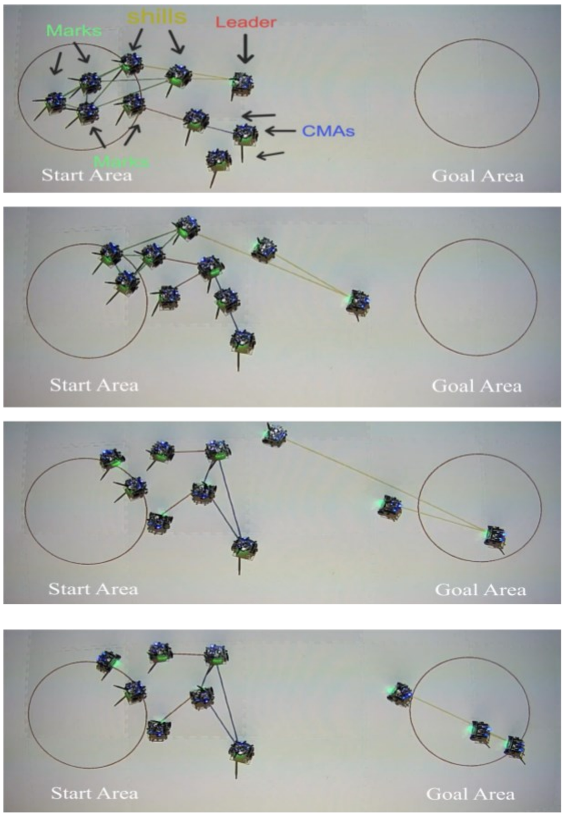

Figure 7. Snapshots of an experiment trial in the Robotarium consisted of four mark robots, two shills, one leader and three CMA robots. The CMAs were abled to form a “barrier” to stop marks misdrected by shills and its leaderfrom reaching the goal area.

VI. CONCLUSION

Misdirection and counter-misdirection have significant potential in the field of mobile robotics, especially for multi-robot systems for possible applications in the military and sports. For instance, one robotic team can use misdirection to draw (feint) its opponent team toward an incorrect location, and the opponent team can use counter-misdirection to deter its members from going there. However, there has been little study on robotic counter-misdirection to date, if any. In this paper, we developed a simple and effective behavior-based counter-misdirection approach for multi-robot teams. We have shown that, by deploying a team of counter-misdirection agents (CMAs), each CMA can estimate a possible intercept location whereby they can form a barrier that uses the fear-based approach to push back misdirected marks thus achieving counter-misdirection. We have also demonstrated the effectiveness of the strategy and investigated its key factors in MissionLab [25]. By deploying a sufficient number of CMAs, they can stop the misdirection process in a range of instances.

In the future, we will create more complex environments to study the applicability of the strategy for more realistic cases, such as adding obstacles.

[1] Video will be posted on https://www.cc.gatech.edu/ai/robot-lab/Deception/.

APPENDIX I

This appendix contains the behavioral assemblages and its composing primitive behaviors for the different types of agents.

TABLE I. THE BEHAVIOR ASSEMBLAGES FOR EACH TYPE OF AGENTS

Type	Behavior Assemblage	Composing Behaviors
Mark	Wander Near Start (Simulation Outset)	*Wander, Stay-Near-Start, Avoid-Obstacle, Off-Robots*
	Mark Mill Around (Below Threshold)	*Wander, Avoid-Obstacle, Off-Robots*
	Mark Flock (Above Threshold)	*Wander, Lek Behavior, Avoid-Obstacle, Color-Pushed-Back, Off-Robots.*
Leader	Lead to Goal	*Go-To-Goal, Avoid-Obstacle, Wander*
Shill	Wander Near Start (Simulation Outset)	*Wander, Stay-Near-Start, Avoid-Obstacle, Off-Robots*
	Shill Flock	*Wander, Follow-Leader, Lek Behavior, Avoid-Obstacle, Off-Robot*
CMA	Wander Near Start (Simulation Outset)	*Wander, Stay-Near-Start, Avoid-Obstacle, Off-Robots.*
	Observe Movement	*Stop, Observe*
	Estimate Intercept Location	*Stop, Estimate-Location*
	Goto Intercept Location	*Goto-Intercept, Color-Pushed-Back, Avoid-Obstacle, Wander.*

Here are the definitions of primitive behaviors in the behavior assemblages; each primitive behavior returns a motion vector. The notation $\hat{v}$ represents the normalized vector of vector $\vec{v}$. In two-dimensional space, $\vec{l} = [x, y]^T$ is used to represent the location of the robot.

Wander (Noise) Behavior: The motion vector makes the robot move in random directions with random speeds, which allows the agent to incorporate realistic noise.

Lek Behavior [10]: This motion vector $\vec{v}_{lek}$ is based on the lek behavior for group formation to let the robot to attract to another robot at location $\vec{l}_r$ where R_A is the radius of the attraction sphere and R_D is the radius of the dead zone sphere.

$$\vec{v}_{lek} = \alpha\hat{v};\ \vec{v} = \vec{l}_r - \vec{l}$$

$$\alpha = \begin{cases} 1 - \dfrac{(R_A - R_D) - (R_A - \|\vec{v}\|)}{(R_A - R_D)} & R_D \le \|\vec{v}\| \le R_A \\ 0 & otherwise \end{cases}$$

Off-Robot Behavior: This motion vector $\vec{v}_{OR}$ prevents the robot from crashing into another robot at location $\vec{l}_r$ given its repulsion sphere R_D.

$$\vec{v}_{OR} = \alpha\hat{v};\ \vec{v} = \vec{l} - \vec{l}_r$$

$$\alpha = \begin{cases} \dfrac{R_r - \|\vec{v}\|}{R_r} & \|\vec{v}\| \le R_r \\ 0 & otherwise \end{cases}$$

Avoid-Obstacle Behavior: This motion vector $\vec{v}_{AO}$ enables the robot with an obstacle avoidance sphere with radius R_{AO} to avoid a known obstacle centered at $\vec{l}_r$ with radius R_o in the environment.

$$\vec{v}_{AO} = \alpha\hat{v};\ \vec{v} = \vec{l} - \vec{l}_r$$

$$\alpha = \begin{cases} \infty & \|\vec{v}\| \le R_o \\ \dfrac{R_{AO} - \|\vec{v}\|}{R_{AO} - R_o} & R_o \le \|\vec{v}\| \le R_{AO} \\ 0 & \|\vec{v}\| > R_{AO} \end{cases}$$

Follow-leader Behavior: This motion vector $\vec{v}_{FL}$ allows the robot to follow its leader at $\vec{l}_l$ if it is within detection range R_L.

$$\vec{v}_{FL} = \alpha\hat{v};\ \vec{v} = \vec{l}_l - \vec{l}$$

$$\alpha = \begin{cases} 1 - \dfrac{R_L - \|\vec{v}\|}{R_L} & \|\vec{v}\| \le R_L \\ 0 & otherwise \end{cases}$$

Go-To-Goal Behavior: Given the goal location $\vec{l}_g$, this vector $\vec{v}_{GG}$ enables the robot to move toward the goal location with an adjustable gain α.

$$\vec{v}_{GG} = \alpha\hat{v};\ \vec{v} = \vec{l}_g - \vec{l}$$

Color-Push-Back Behavior (on mark): The Color-Push-Back vector $\vec{v}_{CPB}$ "pushes" the robots from a predefined-colored robot at $\vec{l}_{color}$ away when it is within the effective area with radius R_e as a fear-based approach with an adjustable fear gain β.

$$\vec{v}_{CPB} = \beta\hat{v};\ \vec{v} = \vec{l} - \vec{l}_{color}$$

$$\beta = \begin{cases} \dfrac{R_e - \|\vec{v}\|}{R_e} & \|\vec{v}\| \le R_r \\ 0 & otherwise \end{cases}$$

Color-Push-Back Behavior (on CMA): The Color-Push-Back vector $\vec{v}_{CPB-CMA}$ "pushes" the CMA from a predefined-colored robot at $\vec{l}_{color}$ along the direction $\hat{b}$ that is perpendicular to the group movement vector $\vec{f}$ based when it is within the effective area with radius R_e as a fear-based approach with an adjustable fear gain β.

$$\vec{v}_{CPB-CMA} = \operatorname{sgn}(\vec{v} \cdot \hat{b})\beta\hat{b};\ \vec{v} = \vec{l} - \vec{l}_{color}$$

$$\hat{b} = \boldsymbol{Rot}(\frac{\pi}{2})\hat{f}$$

$$\beta = \begin{cases} \dfrac{R_e - \|\vec{v}\|}{R_e} & \|\vec{v}\| \le R_r \\ 0 & otherwise \end{cases}$$

APPENDIX II

This appendix contains the counter-misdirection algorithm of a counter-misdirection agent (CMA).

Algorithm 1: The counter-misdirection approach based on linear movment model for each CMA

function Initlization():
  $D = \{\}$
end function

function Movement Observation($\overrightarrow{l_{i,t}}$):
  $D = D \cup \{\overrightarrow{l_{i,t}}\}$
end function

function Intercept Location Estimation($D,\ \gamma$):
  $\vec{c} = [a, b]^T = \sum_{i \in O_T} \overrightarrow{l_{i,\mathrm{T}}}$
  $\vec{f} = [f_x,\ f_y]^T = \sum_{i \in O_T} (\overrightarrow{l_{i,\mathrm{T}}} - \overrightarrow{l_{i,o_i}}) \big/ (T - o_i)$
  $A = (f_x{}^2 + f_y{}^2 - \beta v_{max}^2)$
  $B = (af_x + bf_y)$
  $C = (a^2 + b^2)$
  $m = \max\left\{\frac{-B \pm \sqrt{B^2 - 4AC}}{2A}\right\}$
  $\vec{g} = \frac{\vec{c} + m\vec{f}}{m}$
  $\hat{f} = \frac{\vec{f}}{\|\vec{f}\|}$
  $\hat{b} = \boldsymbol{Rot}(\frac{\pi}{2})\hat{f}$
  $\vec{\imath} = m\vec{g} + \gamma\hat{b}$
  Return $\vec{\imath}\ ,\ \hat{b}$
end function

D: the dataset that contains the locations of 'active' agents' during the CMA's observation.

O_T: the set of 'active' agents that are observed by the CMA at time T.

$\overrightarrow{l_{i,t}}$: the location of agent i at time t.

$\vec{c}$: the centroid of the misdirected group.

$\vec{f}$: the movement vector of the misdirected group.

o_i: the first-time agent i is observed by the CMA.

$\vec{\imath}$: the intercept location for CMA.

m: the time needed for CMA to move to the intercept location $\vec{\imath}$.

$\vec{g}$: the movement vector of the CMA.

$\boldsymbol{Rot}(\cdot)$: a function that produces a 2-dimensional rotation matrix.

$\hat{b}$: unit vector that is perpendicular to the group movement vector $\vec{f}$.

γ: the offset used to calculation the intercept location.

REFERENCES

[1] M. Fowler, A. Thieme, J. Licato, A. Constructivism, and R. Lab, "Robotic Misdirection, for Good Causes Strategically Deceptive Reasoning in Artificial Generally Intelligent Agents."

[2] M. J. Pettinati and R. C. Arkin, "Push and Pull: Shepherding Multi-Agent Robot Teams in Adversarial Situations," in *Proceedings of IEEE Workshop on Advanced Robotics and its Social Impacts, ARSO*, 2019, vol. 2019-Octob, pp. 407–414, doi: 10.1109/ARSO46408.2019.8948797.

[3] A. Dragan, R. Holladay, and S. Srinivasa, "An Analysis of Deceptive Robot Motion," in *Robotics: Science and Systems*, 2015, doi: 10.15607/rss.2014.x.010.

[4] R. C. Arkin, "The Ethics of Robotic Deception."

[5] J. Shim and R. C. Arkin, "A Taxonomy of Robot Deception and Its Benefits in HRI," in *2013 IEEE International Conference on Systems, Man, and Cybernetics*, 2013, pp. 2328–2335, doi: 10.1109/SMC.2013.398.

[6] J. Shim and R. C. Arkin, "Other-oriented Robot Deception: A Computational Approach for Deceptive Action Generation to Benefit the Mark," in *2014 IEEE International Conference on Robotics and Biomimetics (ROBIO 2014)*, 2014, pp. 528–535, doi: 10.1109/ROBIO.2014.7090385.

[7] J. Shim and R. C. Arkin, "The Benefits of Robot Deception in Search and Rescue: Computational Approach for Deceptive Action Selection via Case-based Reasoning," in *2015 IEEE International Symposium on Safety, Security, and Rescue Robotics (SSRR)*, 2015, pp. 1–8, doi: 10.1109/SSRR.2015.7443002.

[8] J. Shim and R. C. Arkin, "Biologically-Inspired Deceptive Behavior for a Robot," in *International Conference on Simulation of Adaptive Behavior*, 2012, pp. 401–411, doi: 10.1007/978-3-642-33093-3_40.

[9] J. Davis and R. Arkin, "Mobbing Behavior and Deceit and Its Role in Bio-inspired Autonomous Robotic Agents," 2012, pp. 276–283.

[10] B. A. Duncan, P. D. Ulam, and R. C. Arkin, "Lek Behavior as a Model for Multi-robot Systems," in *2009 IEEE International Conference on Robotics and Biomimetics (ROBIO)*, 2009, pp. 25–32, doi: 10.1109/ROBIO.2009.5420830.

[11] W. D. Hamilton, "Geometry for the Selfish Herd," 1971.

[12] C. Hartman and B. Benes, "Autonomous Boids," *Comput. Animat. Virtual Worlds*, vol. 17, no. 3–4, pp. 199–206, Jul. 2006, doi: 10.1002/cav.123.

[13] C. W. Reynolds, "Flocks, Herds and Schools: A Distributed Behavioral Model," in *Proceedings of the 14th annual conference on Computer graphics and interactive techniques - SIGGRAPH '87*, 1987, vol. 21, no. 4, pp. 25–34, doi: 10.1145/37401.37406.

[14] M. Granovetter, "Threshold Models of Collective Behavior," *Am. J. Sociol.*, vol. 83, no. 6, pp. 1420–1443, May 1978, doi: 10.1086/226707.

[15] D. Strömbom *et al.*, "Solving the Shepherding Problem: Heuristics for Herding Autonomous, Interacting Agents," doi: 10.1098/rsif.2014.0719.

[16] R. Vaughan, N. Sumpter, J. Henderson, A. Frost, and S. Cameron, "Experiments in Automatic Flock Control," *Rob. Auton. Syst.*, vol. 31, no. 1–2, pp. 109–117, Apr. 2000, doi: 10.1016/S0921-8890(99)00084-6.

[17] P. Nalepka, R. W. Kallen, A. Chemero, E. Saltzman, and M. J. Richardson, "Herd Those Sheep: Emergent Multiagent Coordination and Behavioral-Mode Switching," *Psychol. Sci.*, vol. 28, no. 5, 2017, doi: 10.1177/0956797617692107.

[18] R. Vaughan, N. Sumpter, A. Frost, and S. Cameron, "Robot Sheepdog Project Achieves Automatic Flock Control," *From Anim. To Animat.*, pp. 489–493, 1998.

[19] S. Gade, A. A. Paranjape, and S.-J. Chung, "Herding a Flock of Birds Approaching an Airport Using an Unmanned Aerial Vehicle," in *AIAA Guidance, Navigation, and Control Conference*, 2015, doi: 10.2514/6.2015-1540.

[20] A. A. Paranjape, S.-J. Chung, K. Kim, and D. H. Shim, "Robotic Herding of a Flock of Birds Using an Unmanned Aerial Vehicle," *IEEE Trans. Robot.*, vol. 34, no. 4, pp. 901–915, Aug. 2018, doi: 10.1109/TRO.2018.2853610.

[21] G. Kuhn, H. A. Caffaratti, R. Teszka, and R. A. Rensink, "A psychologically-based taxonomy of misdirection.," *Front. Psychol.*, vol. 5, p. 1392, 2014, doi: 10.3389/fpsyg.2014.01392.

[22] P. Lamont and P. R. R. Wiseman, *Magic in Theory: An Introduction to the Theoretical and Psychological Elements of Conjuring*. Univ of Hertfordshire Press, 2005.

[23] M. J. Pettinati, R. C. Arkin, and A. Krishnan, "Wolves in Sheep's Clothing: Using Shill Agents to Misdirect Multi-Robot Teams."

[24] Ronald C. Arkin, *Behavior-based robotics*. 1998.

[25] G. T. Mobile and R. Laboratory, "MissionLab User Manual for MissionLab version 7.0," 2006.

[26] D. Pickem *et al.*, "The Robotarium: A Remotely Accessible Swarm Robotics Research Testbed," in *2017 IEEE International Conference on Robotics and Automation (ICRA)*, 2017, pp. 1699–1706, doi: 10.1109/ICRA.2017.7989200.